Falkland Island peatland development processes and the pervasive presence of fire

Dmitri Mauquoy[1#], Richard J Payne[2*], Kirill V. Babeshko[3], Rebecca Bartlett[4], Ian Boomer[4], Hannah Bowey[1], Chris D. Evans[5], Fin Ring-Hrubesh[2], David Muirhead[1], Matthew O'Callaghan[4], Natalia Piotrowska[6], Graham Rush[2], Thomas Sloan[2], Craig Smeaton[7], Andrey N. Tsyganov[8,9], Yuri A. Mazei[8,9]

1. Geography and Environment, School of Geosciences, University of Aberdeen, St Mary's Building, Aberdeen AB24 3UF, United Kingdom
2. Environment and Geography, University of York, York YO10 5NG, United Kingdom
3. Department of Zoology and Ecology, Penza State University, 440026, Penza, Russia
4. School of Geography, Earth and Environmental Sciences, University of Birmingham, Edgbaston, Birmingham B15 2TT, United Kingdom
5. Centre for Ecology & Hydrology, Environment Centre Wales, Deiniol Road, Bangor, Gwynedd LL57 2UW, United Kingdom
6. Silesian University of Technology, Institute of Physics-CSE, Gliwice, Poland.
7. School of Geography & Sustainable Development, University of St Andrews, St Andrews, KY16 9AL, UK
8. Department of General Ecology and Hydrobiology, Lomonosov Moscow State University, 119991, Moscow, Russia
9. A.N. Severtsov Institute of Ecology and Evolution RAS, 119071, Moscow, Russia

[#]Corresponding author, d.mauquoy@abdn.ac.uk

*Deceased

Abstract

Palaeoecological analyses of Falkland Island peat profiles have largely been confined to pollen analyses. In order to improve understanding of long-term Falkland Island peat development processes, the plant macrofossil and stable isotope stratigraphy of an 11,550 year Falkland Island *Cortaderia pilosa* (‘whitegrass’) peat profile was investigated. The peatland developed into an acid, whitegrass peatland via a poor fen stage. Macrofossil charcoal indicate that local fires have frequently occurred throughout the development of the peatland. Raman spectroscopy analyses indicate changes in the intensity of burning which are likely to be related to changes in fuel types, abundance of fine fuels due to reduced evapotranspiration/higher rainfall (under weaker Southern Westerly Winds), peat moisture and human disturbance. Stable isotope and thermogravimetric analyses were used to identify a period of enhanced decomposition of the peat matrices dating from ~7020 cal yr BP, which possibly reflects increasing strength of the Southern Westerly winds. The application of Raman spectroscopy and thermogravimetric analyses to the Falkland Island peat profile identified changes in fire intensity and decomposition which were not detectable using the techniques of macrofossil charcoal and plant macrofossil analyses.

Keywords: Holocene; Southern Westerly Winds; Fire; Vegetation Dynamics; Falkland Islands; Raman Spectroscopy; Thermogravimetric Analysis; Testate Amoebae; Charcoal

1 Introduction

The Falkland Islands cover an area of approximately 12,200 km^2 and peatlands there comprise ~40-50% of the total land area (pers. comm. Matt Aitkenhead). The estimated carbon stock of peatlands in the archipelago is ~156 MtC (Payne et al., 2019). The earliest peat deposits date to ~16,500 cal yr years BP (Wilson et al., 2002), therefore Falkland Islands peat deposits have the potential to give insight into long-term carbon processing and storage. They also have the potential to provide palaeoclimate data in order to understand the long-term variability of the Southern Westerly Winds (SWW), given that they lie within the main latitudinal belt (52°S) of the Southern Hemisphere westerly airflow and westerly wind days in the Falkland Islands are the most dominant, with an average of ~180 days per year (Jones et al., 2016). Based upon ERA-79 Interim reanalysis data (1979-2013 CE), there is a positive correlation between the hemispherically averaged Southern Annular Mode (SAM) index and 2–10 m air temperature and wind strength in the Falkland Islands (Turney et al., 2016).

Palaeoclimate data generated from peat profiles in the Falkland Islands can potentially complement the extensive research which has been undertaken in southern South America to detect variability of the SWW (Kilian and Lamy, 2012). However, there are some potential caveats to this, as Falkland Island peat accumulation rates appear to be highly variable which potentially limits their temporal resolution. Payne et al. (2019) recorded low to very low, long-term apparent rates of carbon accumulation in 10 peat profiles collected from the Falkland Islands. This could be due to low initial rates of carbon accumulation or be a consequence of subsequent carbon loss.

Human and associated livestock impacts on the Falkland peats, although now substantial, are limited to the last 250 years; prior to the introduction of cattle, and more recently sheep, there were no native grazing mammals on the islands (Armstrong, 1994). Currently, very little is known about Falkland Island peatland development processes. This is a necessary prerequisite for any peat-based proxy-climate reconstruction, given that peatland autogenic successional changes through time (Hughes et al., 2000) are not solely dependent upon allogenic (climate) forcing.

1.1 Existing palaeoecological reconstructions

A small number of Lateglacial plant macrofossils were identified in peat samples collected from the Lake Sulivan (West Falkland) fan delta (Wilson et al., 2002), but their analysis was not systematically undertaken in the peat deposits investigated. To date only a single, detailed charcoal and plant macrofossil record is available from the Falkland Islands (Hooker's Point), spanning the Pleistocene/Holocene transition (Scaife et al., 2019).

The few palaeoecological reconstructions which have been undertaken in the Falkland Islands have primarily focussed upon the analyses of microfossil pollen, spores and charcoal (Barrow, 1978; Clark et al., 1998; Turney et al., 2016). Palaeoclimate reconstructions based upon changes in Falkland Island pollen spectra have proven to be challenging due to the "...restricted vascular flora, which greatly limits the amount of pollen with climatically diagnostic value" (Clark et al., 1998). To circumvent problems with the low palynological diversity of the indigenous flora (high dominance of *Poaceae* and *Empetrum*), changes in the concentrations of 'exotic', long distance, wind dispersed *Nothofagus*, *Podocarpus*, *Ephedra fragilis* and *Anacardium*-type pollen from southernmost South America (~500 km to the west) have been used as a surrogate for changes in the strength of the SWW (Turney et al., 2016). This same logic was also applied to microfossil charcoal (<106 μm) spectra in the investigated peat profile, given that these too can be transported long distances by the prevailing SWW (Clark, 1988), and potentially offer an indirect measure of past airflow. The 90 cm depth Falkland Island peat profile sequence at

Canopus Hill investigated by Turney et al. (2016) spans the last ~2600 years and a correspondence between microfossil charcoal and *Nothofagus* pollen counts was noted. Both were therefore used as a proxy for long distance transport of these microfossils by stronger SWW winds. Stronger westerly wind flow was identified at 2400, 2100, 1800–1300, 1000, 550 and 250 cal yr BP.

Away from the Falkland Islands, a long period of weaker SWW winds between 8300-4000 cal yr BP was identified in a multi-proxy lake record from eastern Patagonia, ~700 km to the SWW, followed by a re-intensification of the SWW since 3000 cal yr BP (Zolitschka et al., 2019). Conversely, the diatom and ostracod data from Lake Aturo in the semiarid steppe of northern Tierra del Fuego, recorded an increase of salinity with sodium dominated waters due to stronger SWW between 7260-6200 cal yr BP (Fernández et al., 2020).

Based upon the influx of aeolian sand to a peat deposit on Isla de los Estados, easternmost Tierra del Fuego, Björck et al. (2012) identified a period of maximum Holocene SWW strength between 4500-3500 cal yr BP.

Few macrofossil charcoal analyses have been undertaken in the Falkland Islands, but the results of Buckland and Edwards (1998) are noteworthy, in that the basal 50 cm of a peat profile from Sapper Hill, East Falkland contained abundant macrofossil charcoal fragments which were dated to before ~5640-5304 cal yr BP.

The transport distance of macrofossil charcoal is relatively low and can range between several hundreds of metres (Clark et al., 1998; Blackford, 2000; Peters and Higuera, 2007) to tens of kilometers from the depositional archive deposit (Pisaric, 2002; Tinner et al., 2006). The evidence presented by Buckland and Edwards (1998) for *in situ*/local burning of the peat-forming vegetation (*Empetrum rubrum* Vahl ex Willd.) is millennia before the arrival of Europeans (the first French settlement at Port Louis on East Falkland dates to 1764 CE; Armstrong, 1994). The question still remains whether this burning reflects the presence of pre-European humans (travelling from southern South America, either by design or accident?) or natural ignition through lightning strikes, given the relatively low rainfall combined with high flammability of *E. rubrum*, as noted by Hooker (1847), “The stems and leafy branches are much used for fuel in the Falklands where the plant is called “diddle dee”, they are especially employed in kindling fire for even when sodden with rain they speedily ignite and burn with a bright and hot flame”.

The late Quaternary fire history of Patagonia and Tierra del Fuego has been reviewed by Huber et al. (2004). The microfossil charcoals identified in Torres del Paine by Heusser (1995) and in Meseta Latorre I by Schäbitz (1991) both record high fire activity during the entire Holocene. Both of these sites are located in xeric habitats of the steppe-forest ecotone and climatic conditions in these locations during the Holocene “may have always promoted fires” (Huber et al. (2004).

The relationship between ‘unplanned’ fires (including human and lightning ignited fires) in Australia, South Africa and South America and the main Southern Hemisphere climate modes, was explored by Mariani et al. (2018). Based upon these documentary fire records spanning 1958-2014 CE, the Southern Annular Mode (SAM) was identified as the leading climate mode in most of the analysed regions across the Southern Hemisphere. Positive (southward shifted) SAM states were found to be associated with a large increase in the number of fires during the 21st century.

The impacts of burning upon the local peat forming vegetation of Falkland Island peatlands is uncertain, although it is likely that pre-fire weather, peat moisture, water table depth, fuel type and microtopographic position will influence the susceptibility of peat to burning (Bourgeau et al., 2020).

In terms of fire weather, 14 discrete fires on the Falkland Islands were started by lightning strikes between 2000 to 2015 CE, i.e. about one per year on average, although in several cases multiple separate fires were started by a single storm. All lightning strike induced fires occurred between December and April, with most of them in January (Falkland Fire Service data provided by Jim McAdam, pers. comm.).

The effect of lowered water table depth and the vulnerability of northern peatlands to burning was investigated by Turetsky et al. (2011), based upon a long-term peatland drainage experiment in Canada. Carbon losses were found to be nine times higher in the drained plots compared to the pristine plots. In *Sphagnum*-dominated boreal peatlands, accumulation rates decrease significantly with increasing fire frequencies (Kuhry, 1994). The effect of fires in boreal bogs is spatially heterogeneous and dependent upon the microtopographic position (Benscoter et al., 2011). In the blanket bogs of the Falklands, which lack extensive *Sphagnum* cover or typical hummock-hollow microtopography, other factors such as the presence or absence of fire-prone *Empetrum rubrum* (which may in turn reflect peat wetness) could have a greater influence on the spatial development and severity of fires.

1.2 Raman spectroscopy and thermogravimetric analysis

Raman spectroscopy of organic material is a rapid, non-destructive and cost-efficient technique for establishing the thermal maturity of carbonaceous materials. Raman spectroscopy is based upon “Raman scattering” which is due to various elementary excitations where the energy is lost or gained during the scattering process. Given this, Raman spectra can be used as a “fingerprint” for different materials. Analysis of Raman spectra in carbonaceous materials is used to derive the level of thermal maturation of a sample and therefore has the potential to highlight the degree of burning intensity in peatlands. Fossil carbonaceous materials undergo a complex series of reactions when thermally altered, which involve both the formation and reordering of aromatic sub-units towards stacked layers such as graphite. Raman spectroscopy has been widely used (Tuinstra and Koenig 1970; Landis 1971; Nemanich and Solin 1979; Knight and White 1989; Ferrari and Robertson 2001; Beyssac et al. 2002; Muirhead et al., 2012; Muirhead et al., 2017; Muirhead et al.,

2019) as a powerful tool for evaluating the character and thermal alteration of diverse forms of carbonaceous matter (crystalline, nanocrystalline, amorphous). Measurement of spectroscopic parameters are mainly based on two broad first order Raman bands (spectral peaks) at ~1585 cm^{-1} (the graphite peak, G) and ~1350 cm^{-1} (the disorder peak, D). A number of Raman parameters have been developed over the past few decades which involve measurements made on Raman spectral peaks, for example the D/G-peak ratio (I_D/I_G (Intensity [peak height]). Plotting of this ratio can reveal differences in the thermal alteration of the carbonaceous materials (Pasteris and Wopenka, 1991; Jehlička, and Bény 1992). There is agreement that the main changes in the Raman spectra of low maturity organic matter exhibit a narrowing of the G band and an increase of the D band area with thermal maturity increase. Heating experiments based upon Japanese cedar wood and bark charcoal show that the D-band position and the G-band width is dependent upon heat treatment temperature in the region of 400°–800°C (Yamauchi and Kurimoto, 2003).

Thermogravimetric analysis (TGA) can be viewed as both a complex version of loss-on-ignition (LOI, (Dean, 1974; Bengtsson and Enell, 1986)) and a more generic version of rock-eval (Gregorich et al., 2015) and Ramped Pyrolysis (Rosenheim et al., 2008; Rosenheim and Galy, 2012). TGA is a thermal analysis technique in which the mass of a sample is measured over time as temperature ramps upwards at a known rate. TGA is a measure of the whole sample composition. It is not selective and does not require extraction or treatment prior to analysis, unlike other methods such as biomarkers. TGA provides an analytical approach to characterise organic matter (OM) providing information on the quantity, quality and reactivity of the organic fraction. Through the ramped heating process the quality and reactivity of the OM can be determined, in the simplest terms the labile, recalcitrant and refractory components of the OM can be quantified (Capel et al., 2006) and subsequently the biodegradability of the OM can be assessed (Kristensen, 1990).

1.3 Our approach

In this study we apply a suite of established and emerging palaeoecological techniques to a Falkland Island peat profile to determine peatland successional processes through plant macrofossil analysis and to identify whether disturbance through burning is commonplace through the analysis of macrofossil charcoal. We explore the potential of Raman spectroscopy as a technique to identify burning intensity of subfossil char fragments, and TGA to characterise OM preserved in the peat matrices following Lopez-Capel et al. (2005), Plante et al. (2009) and Worrall et al. (2017). Raman spectroscopy has been applied to charcoal deposits preserved in soils (Inoue et al., 2017), but as far as we are aware, has not yet been undertaken on charcoal deposits preserved in peat bogs. TGA has been used to understand the contemporary carbon budget of a blanket peatland (Worrall et al., 2017), but has not yet been systematically applied to peat profile samples in order to identify changes in decomposition through time.

In order to trace precipitation delivery by the SWW we attempt to reconstruct mire surface wetness using testate amoeba assemblages and $\delta^{13}C$ in addition to the plant macrofossil analyses. Testate amoebae are a group of amoeboid protists which produce morphologically distinct shells and are commonly used as surface-moisture proxies in peat-based palaeoclimate studies (Chambers et al., 2012). Changes in testate amoebae assemblages from Tierra del Fuego and southern Patagonia have been used to reconstruct changes in peatbog water table depths on raised *Sphagnum magellanicum* bogs (van Bellen et al., 2016), so there is a possibility that this technique may also provide insight into water table depth changes in Falkland Island peat archive deposits.

2 Materials and methods

The Falkland Island blanket peatlands mainly comprise acid grasslands dominated by *Cortaderia pilosa* (d'Urv.) Hack. and *Empetrum rubrum* dwarf shrub heath (McAdam and Upson, 2012). Cushion (*Astelia pumila* (Forst. f.) Gaudich. and bryophyte bogs (with small patches of *Sphagnum magellanicum* Brid. and *S. fimbriatum* Wilson) are also present within the archipelago, along with the tall tussock-forming tussac grass (*Poa flabellata* (Lam.) Raspail) in ungrazed coastal areas and offshore islands. Falkland peatlands occupy an unusual climatic niche in comparison to Northern Hemisphere peatlands (Loisel and Yu, 2013), with relatively low annual precipitation (~400-600 mm) and temperate conditions with low temperature variability (the mean annual temperature is ~6°C), providing long growing season conditions for the local peat-forming vegetation (Payne et al., 2019).

A 211 cm length peat profile was recovered in 2018 from a whitegrass (*Cortaderia pilosa*) dominated peatland in the Sussex mountains (SSX, 51.63278°S 58.99654°W,) on East Falkland (Fig. 1) using a Russian-pattern peat corer (Aaby and Digerfeldt, 1986). The site is a raised (ombrotrophic) peat dome surrounded by shallow whitegrass peat. The dome of peat is approximately 20 m wide along the E-W axis and 30 m along the N-S axis. There is no erosion along the site margins although a small crescent shape feature on the NW side is perhaps a revegetated erosion scar. Probing indicated similar peat depth throughout and a core was taken from near the point of highest elevation. The upper peat was notably darkly coloured and highly humified. The landscape is fenced pasture land and the site is used for grazing with sheep faeces noted. The nearest fence is c.100 m from the site to the west and a road lies c.100 m to the east. When the peat profile was collected, the peat surface was notably dry with some bare ground. The dominant plant is *E.*

rubrum with *Carex pilosa* Scop., *Blechnum penna-marina* (Poir.) Kuhn, small hummocks of *Bolax gummifera* (Lam.) Sprengel (Balsam Bog), *Myrteola nummularia* (Poir.) O. Berg, *Marsippospermum grandiflorum* (L.f.) Hook. and some *Cladonia* spp. lichens. A total of 43 samples were available for macrofossil analysis from the 211 cm length SSX peat profile. These were warmed in 8% NaOH and sieved (mesh diameter 180 μm). Macrofossils were identified using a binocular microscope (×10–×50) based upon modern type material collected during fieldwork. Identifications were also made with reference to Michaelis (2011) for *Sphagnum* mosses. Volume abundances of all components are expressed as percentages with the exception of fungal fruit bodies, *Carex* spp. nutlets, *Juncus scheuchzerioides* Gaudich. seeds, Acarid mites and macrofossil charcoal fragments, which are presented as the number (n) found in each of the ~5 cm^3 subsamples. Zonation of the macrofossil diagram was made using psimpoll 4.27 (Bennett, 1996), using the optimal splitting by information content option for the LOI, plant macrofossil and macrofossil charcoal data.

Five samples were prepared for AMS ^{14}C dating using an acid-base-acid protocol (Piotrowska, 2013). Samples were disaggregated and inspected under low-powered microscopy before being prepared for AMS ^{14}C dating. The composition of the samples and the ^{14}C dating results after calibration with the SHCal13 calibration curve (Hogg et al., 2013) are presented in Table 1. Chronologies were modelled using a Bayesian approach implemented in the Bacon version 2.3.9.1 package in R (Blaauw and Christen, 2011). In addition, the sampling year 2018 CE was assigned to the surface of the core. After calibration, the modelling procedure of Bacon takes account of the entire probability distribution of each dated level while creating robust chronologies including estimations of age uncertainties. The results of the Bacon derived ^{14}C age/depth modelling are presented in Figure 2.

Sub-samples of ~2 cm^3 volume were ground and incinerated at 550 ºC to calculate LOI. Separate samples for TGA were dried, milled and 20 mg of sample was placed into 70 µl aluminium oxide crucibles. The crucibles were placed into a Mettler Toledo TGA2 (at the University of St Andrews) and heated from 40 to 1000°C at a ramp rate of 10°C min^{-1} under a stream of N_2. The TGA traces were adjusted to be on a common temperature scale and clipped to the range 150 to 650°C to remove interference from absorbed water and inorganic carbon. The TGA traces were normalized to the mass loss, so that all traces were on the same scale and the first derivative of the TGA was calculated (DTG). Finally, the continuous OM mass loss data were grouped into three thermal fractions indicative of OM lability or biodegradability (Capel et al., 2006). These fractions are defined as labile (200-400°C), recalcitrant (400-550°C) and refractory (550-650°C).

For $\delta^{13}C$ analysis, dried samples of bulk sediment were ground to powder, then subsamples of approximately 0.4-0.6 mg were weighed into tin cups and combusted in an Elementar Pyrocube at 920°C. The resulting CO_2 was analysed on an Isoprime Isotope Ratio Mass Spectrometer at the University of Birmingham, Geological Mass Spectrometry Laboratory (GEMS). Internal precision for $\delta^{13}C$ was 0.08 ‰. All samples were replicated with the mean difference between replicates being approximately 0.10 ‰ (range 0.242-0.005 ‰).

Testate amoebae were prepared following the method based on suspension in water, physical agitation and subsequent sedimentation (Mazei and Chernyshov, 2011). The samples were soaked in distilled water for 24 h, agitated on a flask shaker for 30 min, sieved and washed through a 500 µm mesh to remove coarse material and then left to settle for 24 h. The supernatant was decanted away and the samples were mixed with neutralized formaldehyde and placed in glass vials for storage. One milliliter of the concentrated sample was placed in a Petri dish (5 cm diameter), diluted with deionized water if necessary and inspected at ×200 magnification.

Raman measurements of macrofossil charcoal fragments from seven samples (206, 181, 131, 101, 76, 46 and 16 cm core depth) were performed on a Renishaw inVia reflex Raman spectrometer at the University of Aberdeen. Charcoal fragments were picked from the treated macrofossil samples (warmed in 8% NaOH and sieved (mesh diameter 180 µm)) using fine forceps and placed onto a slide. A Leica DMLM reflected light microscope was used to focus the Ar^+ green laser (wavelength 514.5 nm) on 24 different charcoal fragments from each of the samples. The laser spot size was approximately 1-2 µm and laser power between 10-50% (<13 mW power at the sample). The scattered light was dispersed and recorded by means of a CCD (Charge Coupled Device) detector. Data were collected between 1100 cm^{-1} and 1700 cm^{-1} with a spectral resolution less than 3 cm^{-1}. The duration of accumulations was typically up to 10 seconds for between 3 and 5 accumulations. The Renishaw WiRE 3.0 curve-fit software was used for spectral deconvolution. Smoothing and baseline extractions were performed on each sample, including a cubic spline interpolation. Each sample was deconvolved and data extracted at least three times to ensure reproducibility and the removal of any background signal. Peak position and peak full width at half maximum (FWHM) are measured in wavenumbers (cm^{-1}), which records the change in vibrational frequency (stretching and breathing) of the Raman-active carbon molecules. Minimal spectral processing and deconvolution was applied to the measurement of peak areas, with composite G and D bands used to calculate I_D/I_G ratios as outlined in Muirhead et al., (2012; 2017). Prior to analysis of deconvolved spectra, an initial visual approach to spectral interpretation was adopted.

3 Results and interpretation of the proxy data

The degree of preservation of plant macrofossils in the SSX profile is relatively good overall and the entire profile is dominated by undifferentiated graminoids and undifferentiated graminoid roots (Fig. 3, Table 2). Only a very small proportion of the graminoid macrofossils were identifiable to species level (e.g. *Cortaderia pilosa* in zone SSX-5). Relatively low LOI values between 211-206 cm in zone SSX-1 (55% and 67%) indicate the possible in-wash of sediments. The presence of *Carex* spp. nutlets, *Juncus scheuchzerioides* seeds and *Sphagnum magellanicum* leaves and stems in zone SSX-1 (~11,550-8840 cal yr BP) indicate relatively wet and poor-fen conditions (intermediate between fen and bog) during the initial stages of peatland development. Macrofossil charcoal fragments are frequent throughout the peat profile, but relatively low numbers of charcoal fragments were identified in zone SSX-3 (~6590-5470 cal yr BP). The large increase in the amount of unidentifiable organic material in zone SSX-5 (~2820 cal yr BP to the present) suggests that these peat samples are the most decomposed of the entire peat profile.

The preservation of testate amoebae was low with most of the samples recording <10 specimens, with the exception of the samples at depths of 20 cm, 15 cm, 5 cm and the surface sample, where 100+ specimens were identified. A total of 21 taxa were identified, largely dominated by *Assulina muscorum* Greeff, *Corythion dubium* Taranek, *Cryptodifflugia minuta* Playfair, *Cryptodifflugia oviformis* Penard, *Trigonopyxis arcula* Penard, *Trinema lineare* Penard and *Valkanovia delicatula* Valkanov. Poor preservation of testate amoebae is often observed in (poor-) fen peat deposits due to high decomposition rates (Payne, 2011). Given this, it is impossible to infer water table depth based upon the testate amoebae assemblages in the SSX peat profile. Overall, the species composition of testate amoebae in the top layers of the deposits resemble those identified in dry, poor fens (Opravilová and Hájek, 2006).

Representative I_D/I_G ratios and stacked first order Raman spectra are presented in Figures 3 and 4, respectively. There is a distinct narrowing of the G band and increase of the D band widths and intensity (height) (and thus increase of D band area) in three of the samples compared to the others (206 cm, zone SSX-1; 101 cm, zone SSX-2; 16 cm, zone SSX-5). These samples exhibit the greatest I_D/I_G ratios.

The TGA results (Fig. 5) highlight a distinct change in the quantity of the different OM fractions (Capel et al., 2006) at ~103.5 cm (~ 7020 cal yr BP). All three OM fractions increase at 103.5 cm (sample mid-point depth) with the most significant increases observed in the recalcitrant and refractory fractions increasing by ~50% and ~66% respectively.

The SSX carbon stable-isotope profile records an overall depth trend towards lower $\delta^{13}C$ values (Fig. 5) which indicates that accumulation of recalcitrant material depleted in ^{13}C dominates the isotopic profile (Alewell et al., 2011). Changes in $\delta^{13}C$ values along the peat profile are likely to reflect botanical changes to the peat forming vegetation or changes in the extent of decomposition often related to changes in the water table (Nykänen et al., 2018). Four of the most depleted $\delta^{13}C$ values were recorded in zone SSX1 of the peat profile (at mid-point depths of 203.5, 178.5, 168.5 and 163.5 cm). This is likely to reflect the presence of *Carex* spp. in this zone, as these sedges have been found to record relatively depleted $\delta^{13}C$ values between -29.19 to -27.98 ‰ (Skrzypek et al., 2008). A change to relatively enriched $\delta^{13}C$ (-26.81 ‰) occurs at 158.5 cm (~8840 cal yr BP). This may indicate a change in the water chemistry of the peatland (Nykänen et al., 2018) from a poor fen (relatively depleted $\delta^{13}C$) to a bog (relatively enriched $\delta^{13}C$). A second series of depleted $\delta^{13}C$ values were recorded between 103.5-53.5 cm (~7020-4600 cal yr BP), which indicates lower local water table depths with higher rates of decomposition leading to an increased accumulation of ^{13}C depleted compounds such as lignin or phenols (Alewell et al., 2011).

4 Discussion

4.1 Peatland development

The initial peatland development at the SSX site is marked by the presence of *Juncus scheuchzerioides* seeds. This rush is a primary colonizer of bare ground and occurs near pool margins (Upson and Lewis, 2014). The preservation of the *Carex* spp. nutlets was not good enough to allow species level identification, but all of the current 13 *Carex* species in the Falkland Islands grow near standing water or in fen areas (Upson and Lewis, 2014). Abundant leaves of *Sphagnum magellanicum* at the top of the zone suggest that the poor-fen stage persisted until ~8840 cal yr BP, given that this moss occurs in both poor fen (minerotrophic) and bog (acidic, ombrotrophic) peatlands in the Northern/Southern Hemisphere (Kyrkjeeide et al., 2016). The poor-fen zone (SSX-1) extends between ~11,550-8840 cal yr BP during the Southern Hemisphere Early Holocene thermal maximum (11,500-8500 yr BP, Kilian and Lamy, 2012). Multi-proxy palaeoclimate data from Laguna Azul (52°S, 69°W) in south-eastern Patagonia indicate higher precipitation (decreased strength of the SWW) between 11,200-10,199 cal yr BP (Zolitschka et al., 2019). Aeolian sand influx data generated from a peat profile recovered from Isla de los Estados (55°S, 64°W) offers evidence for decreased wind speeds between 12,200-10,000 cal yr BP (Björck et al., 2012). In combination with higher precipitation, the reduced exposure to surface winds may have favoured the initial (semi-) aquatic stages of the initial peatland development. The SSX peatland would not have not been solely rainfed for the first ~3000 years of peat accumulation, so it is not possible to generate a SWW climate reconstruction for this section of the peat profile.

The peat stratigraphy in zones SSX-2 to -4 is relatively homogeneous and indicates the presence of a stable grass bog between ~8840 to ~2820 cal yr BP, which was frequently disturbed by fires. This matches the results recorded for xeric habitats in the steppe-forest ecotone of Patagonia, as these sites also record high fire activity throughout the Holocene (Huber et al., 2004). Preserved grass epidermis tissues were not present, although it is likely that the undifferentiated graminoid and graminoid roots remains are those of *Cortaderia pilosa*. During this long 'ombrotrophic' grass bog stage spanning ~6020 years, it is very difficult to detect changes in mire surface wetness with the plant macrofossil data, given that *Cortaderia pilosa* displays phenotypic plasticity, with a lax morphotype in poorly drained peat and a tussock growth habit in well drained and sheltered areas (Poskuta et al., 1998). The presence of trace amounts of *Sphagnum fimbriatum* leaves in zones SSX-3 and -2 indicates the occurrence of some nutrient 'flushing', given that this minerotrophic species (which has a bipolar global distribution) can grow in moderately calcareous waters (Clymo and Hayward 1982) and is not desiccation tolerant (Green 1968).

In Zone SSX-3 (~6590-5470 cal yr BP) there is a marked reduction in the numbers of charcoal fragments in addition to high numbers of *Cennococcum geophilum* Fr. sclerotia between 86-71 cm (~6250-5580 cal yr BP) and the highest recorded values of *Myrteola nummularia* stems and undifferentiated Ericaceae wood. The increased presence of dwarf shrubs in SSX-3 may be due to the reduced incidence of fires, given that *Empetrum*-dominated ecosystems seem to have low resistance/resilience to fire (Bråthen et al., 2010) possibly due to the sorptive properties of charcoal, which reduce the allelopathic effects of dwarf shrub phenolic compounds (Wardle et al., 1998; Keech et al., 2005). *C. geophilum* (species complex) is a globally ubiquitous ectomycorrhizal fungi (Obase et al., 2017) with 129 species/variations/hybrids of host plants which includes Myrtaceae (Trappe, 1964). *M. nummularia* (Myrtaceae) may have therefore acted as the host plant for *C. geophilum* and its ectomycorrhizae may have served to enhance water uptake by this dwarf shrub (Hasselquist et al., 2005). *C. geophilum* appears to be relatively drought tolerant (Piggot, 1982; Coleman et al., 1989) and its sclerotia can survive long-lasting drought treatments (Glassman et al., 2015; Miyamoto and Nara 2016). Collectively, the macrofossil taxa in zone SSX3 therefore suggest that local water tables depths were relatively low, possibly as a response to increased strength of the SWW (higher rates of evapotranspiration and reduced precipitation, due to the negative correlation between 850-hPa zonal wind speed strength and precipitation in eastern Patagonia (Garreaud et al., 2013)).

In the following zone (SSX-4, ~5470-2820 cal yr BP), *C. geophilum* sclerotia, Ericaceae wood and *M. nummularia* all decrease, which may indicate shallower local water table depths, possibly due to a weakening of the SWW. The most decayed peat matrices (high percentages of unidentifiable organic material) occur in the topmost zone (SSX-5, ~2820 cal yr BP to the present), combined with relatively high amounts of Ericales rootlets. This may indicate another period of low local water tables possibly due to increased SWW strength, impacts of European colonists (Armstrong, 1994) from the eighteenth century to the present (grazing by cattle and sheep), stratospheric ozone depletion over Antarctica (Fogt et al., 2009) or a combination of these factors. Grazing in the Falkland Islands has reduced biomass height, favoured *Empetrum rubrum* over *Cortaderia pilosa*, exposed more bare peat surface, and perhaps also led to increased peat drying due to surface wind exposure. There is a sustained presence of relatively high numbers of macrofossil charcoal fragments and leaves of *Campylopus pyriformis* are present in zone SSX-5. This bryophyte is an early coloniser on burnt peat surfaces (Thomas et al., 1994).

4.2 Fire Regime

With the exception of the surface sample (1cm depth), all of the other samples contained large amounts of macrofossil charcoal fragments which indicate local burning. This contrasts markedly with Thomas et al. (2018), where little/no fire was detected in the local environment of the Canopus Hill peat profile, outside Stanley (based upon micro-charcoal analyses), ~80 km to the east of the SSX peat profile. There may therefore either be a high degree of spatial variability of wildfires in the Falkland Islands, for example due to rainfall gradients (average rainfall is higher in the east, which could have reduced fire frequency at the Canopus Hill site). Alternatively, local burning may not have been detected in the study of Thomas et al. (2018) because macro-charcoal analyses were not undertaken.

The plant macrofossil record indicates that the highest degree of mire surface wetness occurred in zone SSX1, yet despite this, every sample contained large numbers of macrofossil charcoal fragments. Moisture content of organic soils is the single most important property governing the ignition and spread of smouldering peat fires (Rein et al., 2008). One explanation for this is that the SSX peat profile dried out seasonally during this time period, as this would have reduced the moisture content of the above ground fine fuels, making them more likely to burn following lightning strike induced ignition. Lightning activity is low (<0.01 strikes $km^{-2} yr^{-1}$) south of 40°S along the Southern Hemisphere storm track (Virts et al., 2013), but between (~11,550-8840 cal yr BP) enough strikes must have occurred to initiate local burning of the peat bog vegetation. Hunter-gatherers have occupied southern continental Patagonia and Northern Tierra del Fuego since ~11,000 years BP (Miotti et al., 2003; Paunero, 2003; Massone and Prieto, 2004), but the earliest evidence for maritime hunter-gatherer (shell middens) in southern South America currently only extends to 6500 ^{14}C years (Legoupil and Fontugne 1997). Given this, it is unlikely that there could be a human cause for the burning registered in the SSX-1 peat profile, as the timespan of zone SSX-1 predates by millennia the development of seaworthy craft by the ‘canoe people’ (Alacalufe/Kaweskar and Yamana/Yagan), who were skilled navigators and hunted pinnipeds using bark canoes (Morello et al., 2012).

The Raman spectroscopy suggests that the highest intensity fires (indicated by the I_D/I_G ratios and more prominent D bands) occurred in zone SSX-1 at 206 cm, in zone SSX-2 at 101 cm and in zone SSX-5 at 16 cm (Figs. 3 and 4). These higher intensity fires may reflect a combination of favourable fire weather, low fuel moisture contents and for SSX-5, possible human factors (deliberate burning of white grass peatlands) although the likelihood of deliberate fires prior to European settlement in the 1760s CE must be considered low. The highest intensity fires recorded by the Raman spectroscopy at the base of zone SSX-1 may have also resulted from the fuel structure in this section of the peat profile (*J. scheuchzerioides* is only present in SSX-1) during the poor fen stage of peat accumulation. The remaining fires in zones SSX-1 at 181 cm, SSX-2 at 131 cm, SSX-3 at 76 cm and SSX-4 at 46 cm all record relatively lower intensity peat fires. The composition of the peat forming plants and fungi in zone SSX-3 is anomalous and indicates relatively low peat water tables. In northern Patagonia, fire occurrence and spread are promoted by droughts during the fire season (October to April) and also appear to be favoured by above-average moisture conditions during the preceding one to two growing seasons which enhances flammable biomass production (Kitzberger et al., 1997). Low water tables in zone SSX-3 between ~ 6590-5470 cal yr BP may have therefore prevented the build-up of above-ground fine fuels, reducing the intensity of the resulting peat fires. This is supported by the relatively low Raman $\mathrm{I_D/I_G}$ ratios for the sample at 76 cm depth at ~5820 cal yr BP (Fig. 3).

4.3 Changes in the strength of the Southern Westerly Winds?

Detecting water table depth changes as a surrogate for changes in the strength of the Southern Westerly Winds in the grass bog (rain-fed) sections of the SSX peat profile (zones SSX-2 to -4, ~8840 to ~2820 cal yr BP) is difficult due to the poor preservation of the testate amoeba assemblages. However, the increased values of the TGA derived recalcitrant and refractory material in the peat profile (Fig. 5) from ~103.5-53.5 cm (~7020-4600 cal yr BP) and depleted $\delta^{13}C$ values between the same depth interval, suggest that the amount of effective precipitation was reduced from ~7020 cal yr BP, as this is evidence for enhanced peat decay. This could be due to a stronger drying effect of winds and reduced precipitation, given the negative correlation between 850-hPa zonal wind speed strength and precipitation in eastern Patagonia (Garreaud et al., 2013). This also ties in with the results of Saunders et al. (2018) and Fernández et al. (2020) who also found evidence for enhanced Southern Westerly wind strength from ~7000 cal yr BP and ~7250 cal yr BP, respectively. The recalcitrant peat fractions record pronounced changes between (~7020-4600 cal yr BP), which may indicate high variability of the effective precipitation during this time period. The plant macrofossils in zone SSX-3 (6590-5470 cal yr BP) suggest low mire surface wetness due to increased strength of the SWW. Björck et al. (2012) identified two periods of higher wind speeds at 6400 and 5400 cal yr BP in Isla de los Estados, Tierra del Fuego, based upon aeolian sand flux data. Mineral dust flux data from Amsterdam Island record strengthened SWW at the northern edge of the Southern Westerly wind belt (37°S) between 6200 to 4900 cal yr BP (Li et al., 2020). Unfortunately, the quality of the SSX chronology does not match the Björck et al. (2012) and Li et al. (2020) records, which weakens this Falkland Island 'evidence' for SWW variability.

A compounding problem is the low long-term apparent rate of carbon accumulation in the SSX peat profile. This was estimated to be 10.67 g C m^{-2} yr^{-1} (Payne et al. 2019), which is <50% of the figure for the global mean accumulation rate of northern peatlands (Loisel et al., 2014). This is likely to reflect a combination of low initial carbon accumulation of the peat forming vegetation (due to the cool oceanic climate, relatively low precipitation and high wind speeds) and subsequent losses of carbon stocks due to the frequent occurrence of fires. Despite lying at the edge of the climate envelope for global peatlands (Payne et al. 2019), the degree of recalcitrance of Falkland Island peat matrices may well be high in order for peat to have accumulated throughout the Holocene. The highly fibrous nature of *Cortaderia pilosa* (Davies et al., 1990), which is the main Falkland Islands peat builder, may have provided a degree of recalcitrance to the peat litter to permit continued carbon sequestration (Scaife et al., 2019). In future work it would be interesting to measure CO_2 net ecosystem exchange (NEE) fluxes for white grass peat in order to give insight into their CO_2 sink strength.

5 Conclusions

The SSX peat profile has frequently burnt throughout the last ~11,500 years and disturbance through burning is commonplace. This matches fire reconstructions from xeric habitats of the steppe-forest ecotone in southern South America (Huber et al. (2004). Raman spectroscopy builds upon the macrofossil data and offers additional insight into the nature of former burning events which would otherwise be unknown. Higher intensity fires may have occurred due to changes in the production of flammable biomass (abundant fine fuels) due to higher rainfall under weaker SWW winds (SSX-1). Higher intensity fires may also have occurred due to low peat moisture under stronger SWW (recorded by the TGA data) at the top of zone SSX-2 and possible human factors (deliberate burning in zone SSX-5). The observed low peat accumulation rates may have resulted from burning and the persistently low annual precipitation the Falkland Islands received during the course of the Holocene.

The paucity of preserved tests of testate amoebae suggests that water table depths in the grass bog peat profile are likely to have been too low to enable preservation of these organisms. Given this, it is challenging to reconstruct changes in the strength of the SWW using this technique. However, the results of the TGA and $\delta^{13}C$ analyses suggest that a change in the strength of the SWW occurred around ~7020 cal yr BP and that these methods have indicator value in slowly accumulating and fire-disturbed peat profiles.

Acknowledgments

RJP secured funding for this research from the Quaternary Research Association, University of York and the Russian Science Foundation (19-14-00102). We thank Paul Brickle and other members of the South Atlantic Environmental Research Institute for their help with logistics, David Large for valuable discussions about Falkland Islands peat and all landowners for access permission. This work is dedicated to Richard J. Payne who was tragically killed while climbing Peak 6477, a previously unclimbed subsidiary peak of Nanda Devi (Garhwal Himalayas) in May 2019.

References

Aaby, B., Digerfeldt, G. 1986. Sampling Techniques for Lakes and Bogs. In: Berglund, B.E., Ed., Handbook for Holocene Palaeoecology and Palaeohydrology, John Wiley and Sons Ltd., Chichester, 181-194.

Alewell, C., Giesler, R., Klaminder, J., Leifeld, J., Rollog, M. 2011. Stable carbon isotopes as indicators for environmental change in palsa peats. Biogeosciences 8, 1769-1778.

Armstrong, P.H. 1994. Human impact on the Falkland Islands Environment. The Environmentalist 14, 215-231.

Barrow, C. 1978. Postglacial pollen diagrams from south Georgia (sub-Antarctic) and West Falkland island (South Atlantic). J. Biogeogr. 5, 251–274.

Bengtsson, L., Enell, M. 1986. Chemical analysis. In B.E. Berglund (Ed): Handbook of Holocene Palaeoecology and Palaeohydrology, Wiley, Chichester, 423-445 p.

Bennett, K.D. 1996. Determination of the number of zones in a biostratigraphical sequence. New Phytol. 132, 155-170.

Benscoter, B.W., Wieder, R.K. 2003. Variability in organic matter lost by combustion in a boreal bog during the 2001 Chisholm fire. Can. J. For. Res. 33, 2509–2513.

Beyssac, O., Goffé, B., Chopin, C., Rouzaud, J.N. 2002. Raman spectra of carbonaceous material in metasediments: A new geothermometer. J. Metamorph. Geol. 20, 859–871.

Björck, S., Rundgren, M., Ljung, K., Unkel, I., Wallin, A. 2012. Multi-proxy analyses of a peat bog on Isla de los Estados, easternmost Tierra del Fuego: a unique record of the variable Southern Hemisphere Westerlies since the last deglaciation. Quaternary Sci. Rev. 42, 1-14.

Blaauw, M., Christén, J.A. 2011. Flexible paleoclimate age- depth models using an autoregressive gamma process. Bayesian Anal. 6, 457–474.

Blackford, J.J. 2000. Charcoal fragments in surface samples following a fire and the implications for interpretation of subfossil charcoal data. Palaeogeogr. Palaeocl. 164, 33–42.

Bourgeau-Chavez, L.L., Grelik, S.L., Billmire, M., Jenkins, L.K., Kasischke, E.S., Turetsky, M.R. 2020. Assessing boreal peat fire severity and vulnerability of peatlands to early season wildland fire. Front. For. Glob. Change 3, doi: 10.3389/ffgc.2020.00020.

Bråthen, K.A., Fodstad, C.H., Gallet, C. 2010. Ecosystem disturbance reduces the allelopathic effects of *Empetrum hermaphroditum* humus on tundra plants. J. Veg. Sci. 21, 786-795.

Brolly, C., Parnell, J., Bowden, S. 2016. Raman spectroscopy: caution when interpreting organic carbon from oxidizing environments. Planet. Space Sci. 121, 53–59.

Buckland, P. C., Edwards, K. J. 1998. Palaeoecological evidence for possible Pre-European settlement in the Falkland Islands. J. Archaeol. Sci. 25, 599–602.

Capel, E.L., de la Rosa Arranz, J.M., González-Vila, F.J., González-Perez, J.A., Manning, D.A. 2006. Elucidation of different forms of organic carbon in marine sediments from the Atlantic coast of Spain using thermal analysis coupled to isotope ratio and quadrupole mass spectrometry. Org. Geochem. 37, 1983-1994.

Chambers, F.M., Booth, R.K., De Vleeschouwer, F., Lamentowicz, M., Le Roux, G.G., Mauquoy, D., Nichols, J.E., van Geel, B., 2012. Development and refinement of proxy-climate indicators from peats. Quat. Int. 268, 21–33.

https://doi.org/10.1016/j.quaint.2011.04.039.

Clark, J.S. 1988. Particle motion and the theory of charcoal analysis: source area, transport, deposition, and sampling. Quaternary Res. 30, 67–80.

Clark, J.S., Lynch, J.A., Stocks, B.J., Goldammer, J.G. 1998. Relationships between charcoal particles in air and sediments in west-central Siberia. Holocene 8, 19–29.

Clark, R., Huber, U.M., Wilson, P. 1998. Late Pleistocene sediments and environmental change at Plaza Creek, Falkland Islands, South Atlantic. J. Quaternary Sci. 13, 95-105.

Clymo, R.S., Hayward, P.M. 1982. The ecology of *Sphagnum*. In Bryophyte ecology. Edited by A. J. E. Smith. Chapman and Hall, London. pp. 229-289.

Coleman, M.D., Bledsoe, C.S., Lopushinsky, W. 1989. Pure culture response of ectomycorrhizal fungi to imposed water stress. Can. J. Botany 67, 29–39.

Davies, A.B., Riley, J., Walton, D.W.H. 1990. Plant form, tiller dynamics and above-ground standing crops of the range of *Cortaderia pilosa* communities in the Falkland Islands. J. Appl. Ecol. 27, 298-307.

Dean, J.W.E. 1974. Determination of carbonate and organic matter in calcareous sediments and sedimentary rocks by loss on ignition: comparison with other methods. J. Sediment. Petrol. 44, 242-248.

Fernández, M., Ponce, J.F., Ramón Mercau, J., Coronato, A., Laprida, C., Maidana, N., Quiroga, D., Magneres, I. 2020. Paleolimnological response to climate variability during Late Glacial and Holocene times: A record from Lake Arturo, located in the Fuegian steppe, southern Argentina. Palaeogeogr. Palaeocl., https://doi.org/10.1016/j.palaeo.2020.109737

Ferrari, A.C., Robertson, J. 2001. Resonant Raman spectroscopy of disordered, amorphous and diamond- like carbon. Phys. Rev. *B* 64, 075414.

Fogt, R.L., Perlwitz, J., Monaghan, A.J., Bromwich, D.H., Jones, J.M., Marshall, G.J. 2009. Historical SAM variability. Part II: Twentieth-Century variability and trends from reconstructions, observations, and the IPCC AR4 models. J. Climate 22, 5346–5365.

Garreaud R., Lopez P., Minvielle M., Rojas, M. 2013. Large-scale control on the Patagonian climate. J. Climate 26, 215–230.

Glassman, S.I., Peay, K.G., Talbot, J.M., Smith, D.P., Chung, J.A., Taylor, J.W., Vilgalys, R., Bruns, T.D. 2015. A continental view of pine-associated ectomycorrhizal fungal spore banks: a quiescent functional guild with a strong biogeographic pattern. New Phytol. 205, 1619–1631.

Green, B. H. 1968. Factors influencing the spatial and temporal distribution of *Sphagnum imbricatum* Homsch. ex Russ. in the British Isles. J. Ecol. 56, 47-58.

Gregorich, E.G., Gillespie, A.W., Beare, M.H., Curtin, D., Sanei, H., Yanni, S.F. 2015. Evaluating biodegradability of soil organic matter by its thermal stability and chemical composition. Soil Biol. Biochem. 91, 182–191.

Hasselquist N., Germino M.J., McGonigle T., Smith W.K. 2005. Variability of *Cenococcum* colonization and its ecophysiological significance for young conifers at alpine-treeline. New Phytol. 165, 867–873.

Heusser, C.J. 1995. Three late Quaternary pollen diagrams from Southern Patagonia and their palaeoecological implications. Palaeogeogr. Palaeocl. 118, 1-24.

Hogg A.G., Hua Q., Blackwell P.G., Niu, M., Buck, C.E., Guilderson, T.P., Heaton, T.J., Palmer, J.G., Reimer, P.J., Reimer, R.W., Turney, C.S.M., Zimmerman, S.R.H. 2013. SHCal13 Southern Hemisphere calibration, 0–50,000 years cal BP. Radiocarbon 55, 1889-1903.

Hooker, J.D. 1847. The botany of the Antarctic voyage of H.M. Discovery Ships Erebus and Terror in the Years 1839-1843. Under the command of Captain Sir James Clark Ross. Reeve Brothers, London.

Huber, U.M., Markgraf, V., Schäbitz, F. 2004. Geographical and temporal trends in Late Quaternary fire histories of Fuego-Patagonia, South America. Quaternary Sci. Rev. 23, 1079-1097.

Hughes, P.D.M., Mauquoy, D., Barber, K.E., Langdon, P.G. 2000. Mire-development pathways and palaeoclimatic records from a full Holocene peat archive at Walton Moss, Cumbria, England. Holocene 10, 465–479.

Inoue, Yoshie, A., Tanaka, T., Onji, T., Inoue, Y. 2017. Disappearance and alteration process of charcoal fragments in cumulative soils studied using Raman spectroscopy. Geoderma 285, 164-172.

Jehlička, J. and Bény, C. 1992. Application of Raman microspectrometry in the study of structural changes in Precambrian kerogens during regional metamorphism. Org. Geochem. 18, 211–213.

Jones, P.D., Harpham, C., Lister, D. 2016. Long-term trends in gale days and storminess for the Falkland Islands. Int. J. Climatol. 36, 1413-1427.

Keech, O., Carcaillet, C., Nilsson, M.C. 2005. Adsorption of allelopathic compounds by wood-derived charcoal: the role of wood porosity. Plant Soil 272, 291–300.

Kilian, R., Lamy, F. 2012. A review of Glacial and Holocene paleoclimate records from southernmost Patagonia (49-55°S). Quaternary Sci. Rev. 53, 1-23.

Kitzberger, T., Veblen, T.T., Villalba, R. 1997. Climatic influences on fire regimes along a rain forest-to-xeric woodland gradient in northern Patagonia, Argentina. J. Biogeogr. 24, 35-47.

Knight, D.S., White, W.B. 1989. Characterization of diamond films by Raman spectroscopy. J. Mater. Res. 4, 385–393.

Kristensen, E., 1990. Characterization of biogenic organic matter by stepwise thermogravimetry (STG). Biogeochemistry 9,135-159.

Kuhry, P. 1994. The role of fire in the development of *Sphagnum*-dominated peatlands in western boreal Canada. J. Ecol. 82, 899-910.

Kyrkjeeide, M. O., Hassel, K., Flatberg, K.I., Shaw, A.J., Yousefi, N., Stenøien, H.K. 2016. Spatial Genetic Structure of the Abundant and Widespread Peatmoss

Sphagnum magellanicum Brid. PLoS ONE 1111: e0148447. doi:10.1371/journal. pone.0148447</Info

Landis C.A. 1971. Graphitisation of dispersed carbonaceous material in metamorphic rocks. Contrib. Mineral. Petr. 30, 34-45.

Legoupil, D., Fontugne, R. 1997. El poblamiento marítimo en los archipiélagos de Patagonia: núcleos antiguos y dispersión reciente. Anales del Instituto de la Patagonia. Serie Ciencias Humanas 25, 75-87.

Li, C., Sonke, J.E., Le Roux, G., Van der Putten, N., Piotrowska, N., Jeandel, C., Mattielli, N., Benoit, M., Wiggs, G.S.F., De Vleeschouwer, F. 2020. Holocene dynamics of the southern westerly winds over the Indian Ocean inferred from a peat dust deposition record. Quat. Sci. Rev. 231, https://doi.org/10.1016/j.quascirev.2020.106169

Loisel, J., Yu, Z., Beilman, D.W., Camill, P., Alm, J., Amesbury, M.J., Anderson, D., Andersson, S., Bochicchio, C., Barber, K., Belyea, L.R., Bunbury, J., Chambers, F.M., Charman, D.J., De Vleeschouwer, F., Fiałkiewicz-Kozieł, B., Finkelstein, S.A., Gałka, M., Garneau, M., Hammarlund, D., Hinchcliffe, W., Holmquist, J., Hughes, P., Jones, Klein, E.S., Kokfelt, U., Korhola, A., Kuhry, P., Lamarre, A., Lamentowicz, M., Large, D., Lavoie, M., MacDonald, G., Magnan, G., Mäkilä, M., Mallon, G., Mathijssen, P., Mauquoy, D., McCarroll, J., Moore, T.R., Nichols, J., O’Reilly, B., Oksanen, P., Packalen, M., Peteet, D., Richard, P.J.H., Robinson, S., Ronkainen, T., Rundgren, M., Sannel, A.B.K., Tarnocai, C., Thom, T., Tuittila, E.-S., Turetsky, M., Väliranta, M., van der Linden, M., van Geel, B., van Bellen, S., Vitt, D., Zhao, Y., Zhou, W. 2014. A database and synthesis of northern peatland soil properties and Holocene carbon and nitrogen accumulation. Holocene 24, 1028-1042.

Loisel, J., Yu, Z. 2013. Holocene peatland carbon dynamics in Patagonia. Quaternary Sci. Rev. 69, 125-141.

Lopez-Capel, E., Sohi, S.P., Gaunt, J.L., Manning, D.A. 2005. Use of thermogravimetry–differential scanning calorimetry to characterize modelable soil organic matter fractions. Soil Sci. Soc. Am. J. 69, 136-140.

Mariani, M., Holz, A., Veblen, T.T., Williamson, G., Fletcher, M.-S., Bowman, D.M.J.S. 2018. Climate change amplifications of climate-fire teleconnections in the Southern Hemisphere. Geophys. Res. Lett. 45, https://doi.org/10.1029/2018GL078294.

Massone, M., Prieto, A. 2004. Evaluación de la Modalidad Cultural Fell 1 en Magallanes. Chungará 36 (suppl.): 303–315.

Mazei, Y.A., Chernyshov, V.A. 2011. Testate amoebae communities in the southern tundra and forest-tundra of Western Siberia. Biology Bull. 38, 789–796.

McAdam, J.H., Upson, R. 2012. Peatlands in the Falkland Islands – Origins, status and threats. IUCN UK Peatland Programme/British Ecological Society Symposium, Bangor Wales. p15.

Michaelis, *D.* 2011*.* Die *Sphagnum*-Arten der Welt. Bibliotheca Botanica 160, Schweizerbart Science Publishers, Stuttgart, 408 pp. (in German).

Miotti, L., Salemme, M., Rabassa, J. 2003. Radiocarbon chronology at Piedra Museo locality. In: Miotti, L., Salemme, M., Flegenheimer, N. (Eds.), Where the South Winds

Blow. Centre for the Study of First Americans and Texas A and M University Press, Texas, 99-104.

Miyamoto, Y., Nara, K. 2016. Soil propagule banks of ectomycorrhizal fungi share many common species along an elevation gradient. Mycorrhiza 26, 189–197.

Morello, F., Borrero, L., Massone, M., Stern, C., García-Herbst, A., McCulloch, R., Arroyo-Kalin, M., Calás, E., Torres, J., Prieto, A., Martinez, I., Bahamonde, G., Cárdenas, P. 2012. Hunter-gatherers, biogeographic barriers and the development of human settlement in Tierra del Fuego. Antiquity 86, 71-87

Muirhead, D.K., Parnell, J., Taylor, C., Bowden, S.A. 2012. A kinetic model for the thermal evolution of sedimentary and meteoritic organic carbon using Raman spectroscopy. J. Anal. Appl. Pyrol. 96, 153–161.

Muirhead, D.K., Parnell, J., Spinks, S., Bowden, S.A. 2017. Characterization of organic matter in the Torridonian using Raman spectroscopy. Geol. Soc. Spec. Publ. 448, 71-80.

Muirhead, D.K., Bond, C.E., Watkins, H., Butler, R.W., Schito, A., Crawford, Z. and Marpino, A. 2019. Raman Spectroscopy: an effective thermal marker in low temperature carbonaceous fold-thrust belts. Geol. Soc. Spec. Publ. 490, doi: 10.1144/SP490-2019-27.

Nemanich, R.J., Solin, S.A. 1979. First and second order Raman scattering from finite-size crystals of graphite. Phys. Rev. *B*, 20, 392–401.

Nykänen, N., Mpamah, P.A., Rissanen, A.J. 2018. Stable carbon isotopic composition of peat columns, subsoil and vegetation on natural and forestry drained boreal peatlands. Isot. Environ. Healt. S. 54, 622-641, DOI:10.1080/10256016.2018.1523158.

Obase, K., Douhan, G.W., Matsuda, Y., Smith, M.E. 2017. Progress and Challenges in Understanding the Biology, Diversity, and Biogeography of *Cenococcum geophilum*. In: Tedersoo L. (eds) Biogeography of Mycorrhizal Symbiosis. Ecological Studies (Analysis and Synthesis), vol. 230. Springer, Cham.

Opravilová, V., Hájek, M. 2006. The variation of testacean assemblages (Rhizopoda) along the complete base-richness gradient in fens: a case study from the western Carpathians. Acta Protozool. 45, 191-204.

Pasteris J. D., Wopenka, B. 1991. Raman spectra of graphite as indicators of degree of metamorphism. Can. Minerol. 29, 1-9.

Paunero, R., 2003. The Cerro Tres Tetas (C3T) locality in the central plateau of Santa Cruz, Argentina. In: Miotti, L., Salemme, M., Flegenheimer, N. (Eds.), Where the South Winds Blow. Centre for the Study of First Americans and Texas A and M University Press, Texas, 133-140.

Payne, R.J. 2011. Can testate amoeba-based palaeohydrology be extended to fens? J. Quaternary Sci. 26, 15–27.

Payne, R.J., Ring-Hrubesh, F., Rush, G., Sloan, T.J., Evans, C.D. and Mauquoy, D. 2019. Peatland initiation and carbon accumulation in the Falkland Islands. Quaternary Sci. Rev. 212, 213-218.

Peters, M.E., Higuera, P.E. 2007. Quantifying the source area of macroscopic charcoal with a particle dispersal model. Quaternary Res. 67, 304-310.

Piggott C.D. 1982. Survival of mycorrhiza formed by *Cenococcum geophilum* Fr. in dry soils. New Phytol. 92, 513–517.

Piotrowska, N. 2013. Status report of AMS sample preparation laboratory at GADAM Centre, Gliwice, Poland. Nucl. Instrum. Methods Phys. Res. B 294, 176-181. https://doi.org/10.1016/j.nimb.2012.05.017

Pisaric, M.F.J. 2002. Long-distance transport of terrestrial plant material by convection resulting from forest fires. J. Paleolimnol. 28, 349–354.

Plante, A. F., Fernandez, J. M., Leifeld, J. 2009. Application of thermal analysis techniques in soil science. Geoderma 153, 1–10, doi:10.1016/j.geoderma.2009.08.016.

Poskuta, J.W., McAdam, J.H., Wacławczyk-Lach, E., Wróbleska, B. 1998. Photosynthetic and Respiratory Characteristics of Cortaderia pilosa (D'Urv.) Hack., the Dominant Component of Falkland Islands. J. Plant Physiol. 153, 517-519.

Rein G., Cleaver N., Ashton C., Pironi P., Torero J. L. 2008. The severity of smouldering peat fires and damage to the forest soil. Catena 74, 304-309.

Rosenheim B.E., Day, M.B., Domack, E., Schrum, H., Beenthien, A., Hayes, J.M. 2008. Antarctic sediment chronology by programmed-temperature pyrolysis:

methodology and data treatment. Geochem. Geophy. Geosy. 9, doi:10.1029/2007GC001816.

Rosenheim, B.E., Galy, V. 2012. Direct measurement of riverine particulate organic carbon age structure. Geophys. Res. Lett. 39, doi:10.1029/2012GL052883.

Rouzaud, J.N., Oberlin, A., Beny-Bassez, C. 1983. Carbon films: Structure and microtexture (optical and electron microscopy, Raman spectroscopy). Thin Solid Films 105, 75–96.

Saunders, K.M., Roberts, S.J., Perren, B., Butz, C., Sime, L., Davies, S., Van Nieuwenhuyze, W., Grosjean, M., Hodgson, D.A. 2018. Holocene dynamics of the Southern Hemisphere westerly winds and possible links to CO_2 outgassing. Nat. Geosci. 11, 650-655.

Scaife, R.G., Long, A.J., Monteath, A.J., Hughes, P.D.M., Bentley, M.J., Stone, P. 2019. The Falkland Islands' palaeoecological response to millennial-scale climate perturbations during the Pleistocene–Holocene transition: Implications for future vegetation stability in the southern ocean islands. J. Quaternary Sci., DOI: 10.1002/jqs.3150.

Schäbitz, F. 1991. Holocene vegetation and climate in southern Santa Cruz, Argentina. Bamberger Geographische Schriften 11, 235-244.

Skrzypek, G., Paul, D., Wojtun, B. 2008. Stable isotope composition of plants and peat from Arctic mire and geothermal area in Iceland. Pol. Polar Res. 29, 365–376.

Thomas, P.A., Proctor, M.C.F., Maltby, E. 1994. The ecology of severe moorland fire on the North York Moors: chemical and physical constraints on moss establishment from spores. J. Ecol. 82, 457-474.

Thomas, Z.A., Jones, R.T., Fogwill, C.J., Hatton, J., Williams, A.N., Hogg, A., Mooney, S., Jones, P., Lister, D., Mayewski, P., Turney, C.S.M. 2018. Evidence for increased expression of the Amundsen Sea Low over the South Atlantic during the late Holocene. Clim. Past 14, 1727-1738.

Tinner, W., Hofstetter, S., Zeugin, F., Conedera, M., Wohlgemuth, T., Zimmermann, L., Zweifel, R. 2006. Long-distance transport of macroscopic charcoal by an intensive crown fire in the Swiss Alps—implications for fire history reconstruction. Holocene 16, 287–292.

Trappe J.M. 1964. Mycorrhizal host and distribution of *Cenococcum graniforme.* Lloydia 27, 100–106.

Tuinstra, F., Koenig, J.L. 1970. Raman spectrum of graphite. *Chem. Phys. 53*, 1126–1130.

Turetsky, M.R., Donahue, W.F., Benscoter, B.W. 2011. Experimental drying intensifies burning and carbon losses in a northern peatland. Nat. Commun. 2, doi: 10.1038/ncomms1523.

Turney C.S.M., Jones R.T., Fogwill C., Hatton, J., Williams, A.N., Hogg, A., Thomas, Z.A., Palmer, J., Mooney, S., Reimer, R.W. 2016. A 250-year periodicity in Southern Hemisphere westerly winds over the last 2600 years. Clim. Past 12, 189–200.

Upson R and Lewis R. 2014. Updated atlas and checklist. Report to Falklands Conservation. 226 pp.

van Bellen, S., Mauquoy, D., Hughes, P.D.M., Roland, T.P., Daley, T.J., Loader, N.J., Street-Perrott, F.A., Rice, E.M., Pancotto, V.A., Payne, R.J. 2016. Late-Holocene climate dynamics recorded in the peat bogs of Tierra del Fuego, South America. Holocene 26, 489-501.

Virts, K.S., Wallace, J.M., Hutchins, M.L., Holzworth, R.H. 2013. Highlights of a new ground-based, hourly global lightning climatology. B. Am. Meteorol. Soc. 94, 1381-1391.

Wardle, D.A., Zackrisson, O., Nilsson, M.C. 1998. The charcoal effect in boreal forests: mechanisms and ecological consequences. Oecologia 115, 419–426.

Wilson, P., Clark, R., Birnie, J., Moore, D.M. 2002. Late Pleistocene and Holocene landscape evolution and environmental change in the Lake Sulivan area, Falkland Islands, South Atlantic. Quaternary Sci. Rev. 21, 1821–1840.

Worrall, F., Moody, C.S., Clay, G.D., Burt, T.P., Rose, R., 2017. The flux of organic matter through a peatland ecosystem: The role of cellulose, lignin, and their control of the ecosystem oxidation state. J. Geophys. Res.- Biogeo. 122, 1655-1671.

Yamauchi, S., Kurimoto, Y. 2003. Raman spectroscopic study on pyrolyzed wood and bark of Japanese cedar: temperature dependence of Raman parameters. J. Wood Sci. 49, 235-240.

Zolitschka, B., Fey, M., Janssen, S., Maidana, N. I., Mayr, C., Wulf, S., Haberzettl, T., Corbella, H., Lücke, A., Ohlendorf, C., Schäbitz, F. Southern Hemispheric Westerlies control sedimentary processes of Laguna Azul (south-eastern Patagonia, Argentina). Holocene 29, 402-420.

Lab ID	Depth (cm)	^{14}C age (BP)	Sample composition	Calibrated age ranges (cal yr BP)	Modelled age (cal yr BP)
GdA-5971	21	2535±25	Charcoal fragments and above-ground graminoid leaf fragments	68.2% probability 2740 (39.7%) 2700 2630 (10.2%) 2620 2585 (4.5%) 2575 2560 (13.8%) 2540 95.4% probability 2740 (43.9%) 2690 2635 (12.6%) 2615 2590 (38.9%) 2500	2580±90
GdA-5972	71	4875±30	Fungal fruit bodies (*Cenococcum* spp. sclerotia)	68.2% probability 5640 (19.2%) 5630 5610 (49.0%) 5590 95.4% probability 5655 (95.4%) 5585	5585±100
GdA-5974	131	7365±30	Charcoal fragments and above-ground graminoid leaf fragments	68.2% probability 8300 (17.9%) 8260 8210 (38.2%) 8160 8110 (0.7%) 8120 8090 (11.5%) 8060 95.4% probability 8310 (95.4%) 8050	8170±90
GdA-5973	161	7885±30	*Sphagnum magellanicum* leaves, stems and branches	68.2% probability 8740 (3.2%) 8740 8720 (65.0%) 8600 95.4% probability 8970 (5.9%) 8920 8900 (1.1%) 8890 8860 (4.9%) 8830 8790 (83.5%) 8590	8850±120
D-AMS-029686	211	10,090±30	Above-ground graminoid leaf fragments	68.2% probability 11760 (65.7%) 11610 11520 (2.5%) 11510 95.4% probability 11930 (2.3%) 11890 11820 (76.6%) 11590 11570 (16.5%) 11410	11560±210

Table 1. Details and results of dated subsamples. Depth refers to the position of the centre of each subsample.

Macrofossil zone	**Depth (cm)**	**Age (cal yr BP)**	**Main features**
SSX-5	23.5-1 cm	2820-present	Marked increase in the percentage abundances of unidentifiable organic material, with peak values of 72% at 16 cm depth. Relatively high values of Ericales rootlets. The sample at 1 cm depth contains abundant *Campylopus pyriformis* leaves. Relatively high charcoal fragments between 16-6 cm. LOI decreases between 16-6 cm (86.5 to 83% respectively).
SSX-4	68.5-23.5 cm	5470-2820	Increase in the number of charcoal fragments with maxima at 61 cm and between 46-36 cm. Charcoal fragments decrease towards the top of the zone (31-26 cm). Ericales rootlets are consistently present between 46-26 cm.
SSX-3	93.5-68.5 cm	6590-5470	Marked reduction in the number of charcoal fragments. The highest numbers/percentages of *Cennococcum geophilum*, cf. Type 8 fruit bodies, *Myrteola nummularia* stems and Ericaceae wood were recorded in this zone.
SSX-2	158.5-93.5 cm	8840-6590	The peat matrices are dominated by undifferentiated graminoids and graminoid roots. Relatively high values of Ericales rootlets (~13%) were recorded at 151 cm. Sporadic presence of *Sphagnum fimbriatum* leaves (~1% only). Constant charcoal throughout, but the highest number occur between 141-121 cm. Reduced charcoal present between 116-106 cm.
SSX-1	211-158.5 cm	11,550-8840	Relatively low LOI values between 211-206 cm (55% and 67% respectively. High numbers of *Juncus scheuchzerioides* seeds at the base of the profile, followed by relatively high numbers of *Carex* spp. nutlets. High values (up to 84%) of *Sphagnum magellanicum* at the top of the zone. Relatively high numbers of charcoal fragments present between 206-201 cm and 186-181 cm. Reduced charcoal present between 176-161 cm.

Table 2 Macrofossil zonation for the SSX profile

Figure captions:

Fig. 1: **a**. location of the Falkland Islands/Islas Malvinas in the South Atlantic Ocean, **b**. site locations: Sussex Mountains (SSX, 58.99654°W, 51.63278°S) peat profile (black triangle), other sites mentioned in the text (black squares), Canopus Hill (Turney et al., 2016), Hooker's Point (Scaife et al., 2019), Lake Sulivan (Wilson et al., 2002), Sapper Hill (Buckland and Edwards (1998) **c**. photograph of the SSX peat profile coring location.

Fig. 2: Bacon age depth model. The accumulation rate prior was set to 50 years cm^{-1} with a shape of 1.5. The memory prior was set to a strength of 4 and a mean of 0.7. The model is based upon 43 sections (5 cm thick).

Fig. 3: SSX loss-on-ignition and plant macrofossils. Volume abundances of all components are expressed as percentages with the exception of seeds, nutlets, fungal fruit bodies/sclerotia and charcoal fragments, which are presented as the number (n) found in each ~ 5 cm^3 subsample. The highest 3 Raman Intensity ratios (I_D/I_G) bars are filled with red, the remainder (lower I_D/I_G ratios) are filled with orange. The zonation is based upon the loss-on-ignition, plant macrofossil and macrofossil charcoal data.

Fig. 4: Raman scattering intensity vs. Raman shifts. D = disorder peak, G = graphite peak. The three highest intensity fires from the seven samples (at 206, 101 and 16 cm depth) are filled with red, the remainder indicate lower intensity fires (filled with orange).

Fig. 5: $\delta^{13}C$ and TGA, OM mass loss data grouped into three thermal fractions: labile (200-400°C), recalcitrant (400-550°C) and refractory (550-650°C). The zonation is based upon the loss-on-ignition, plant macrofossil and macrofossil charcoal data.

Figure 1

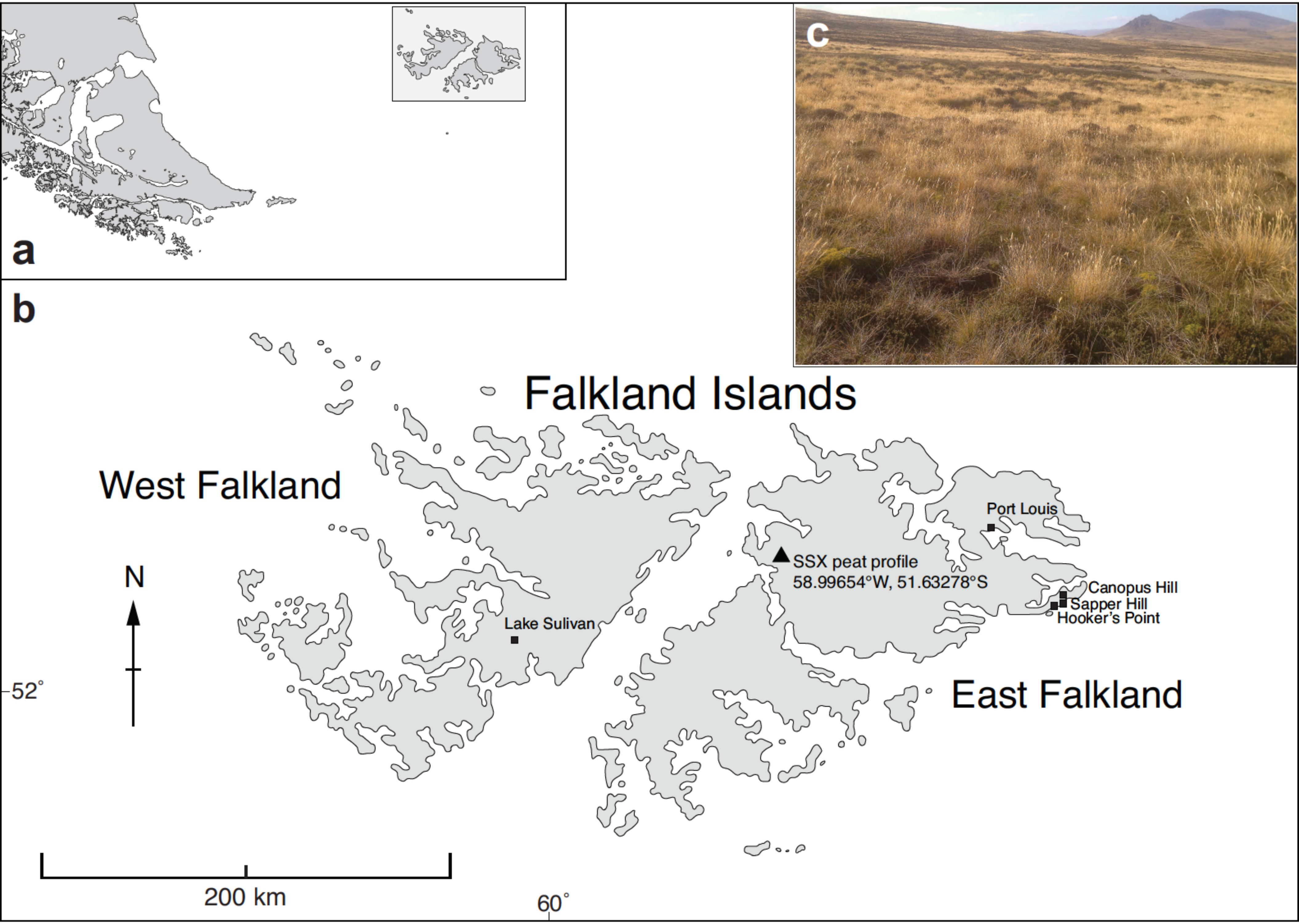
a
c
b
Falkland Islands
West Falkland
East Falkland
Port Louis
SSX peat profile
58.99654°W, 51.63278°S
Canopus Hill
Sapper Hill
Hooker's Point
Lake Sulivan
N
52°
200 km
60°

Figure 2

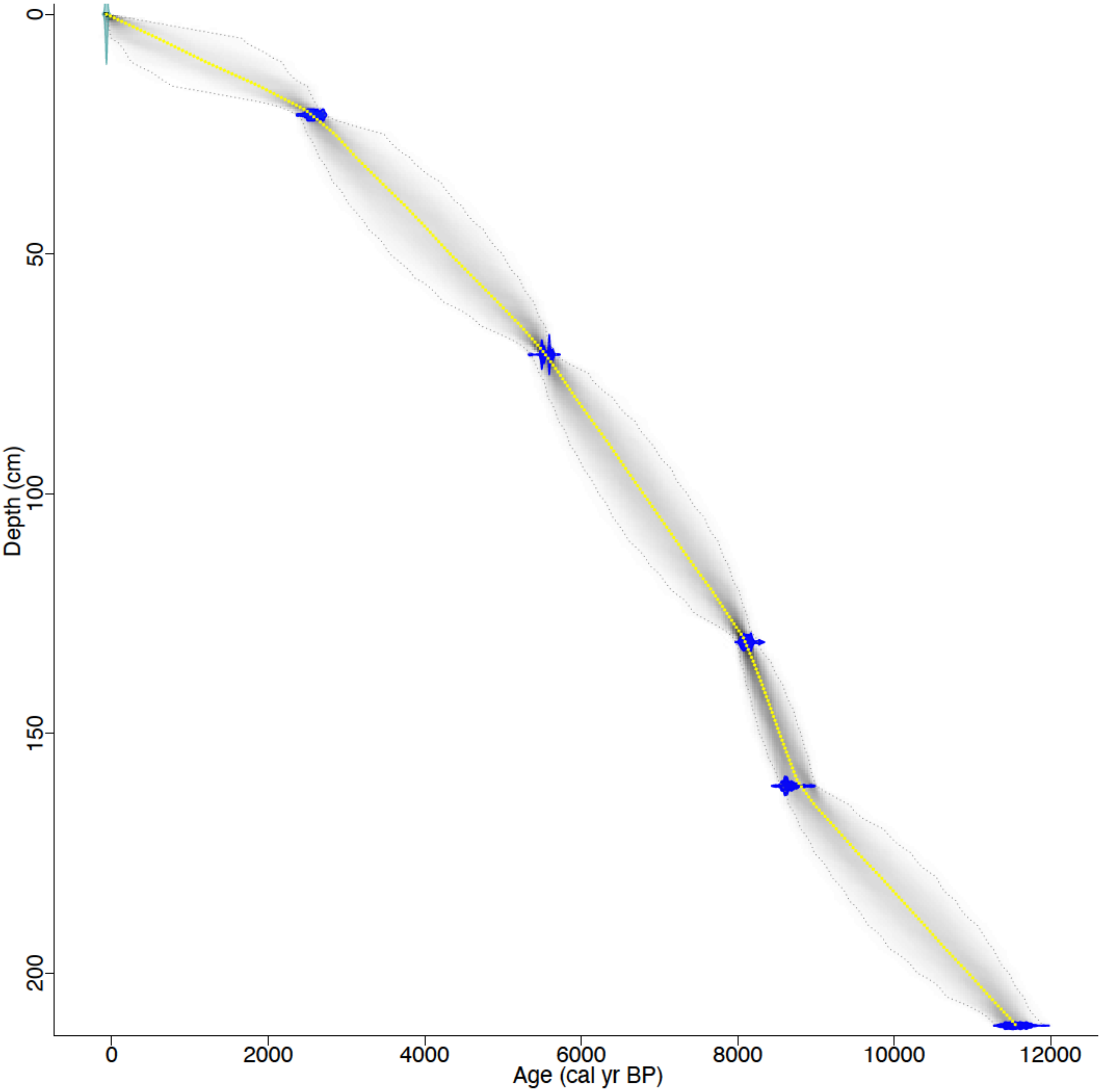
Depth (cm)
0
50
100
150
200
Age (cal yr BP)
0
2000
4000
6000
8000
10000
12000

Figure 3

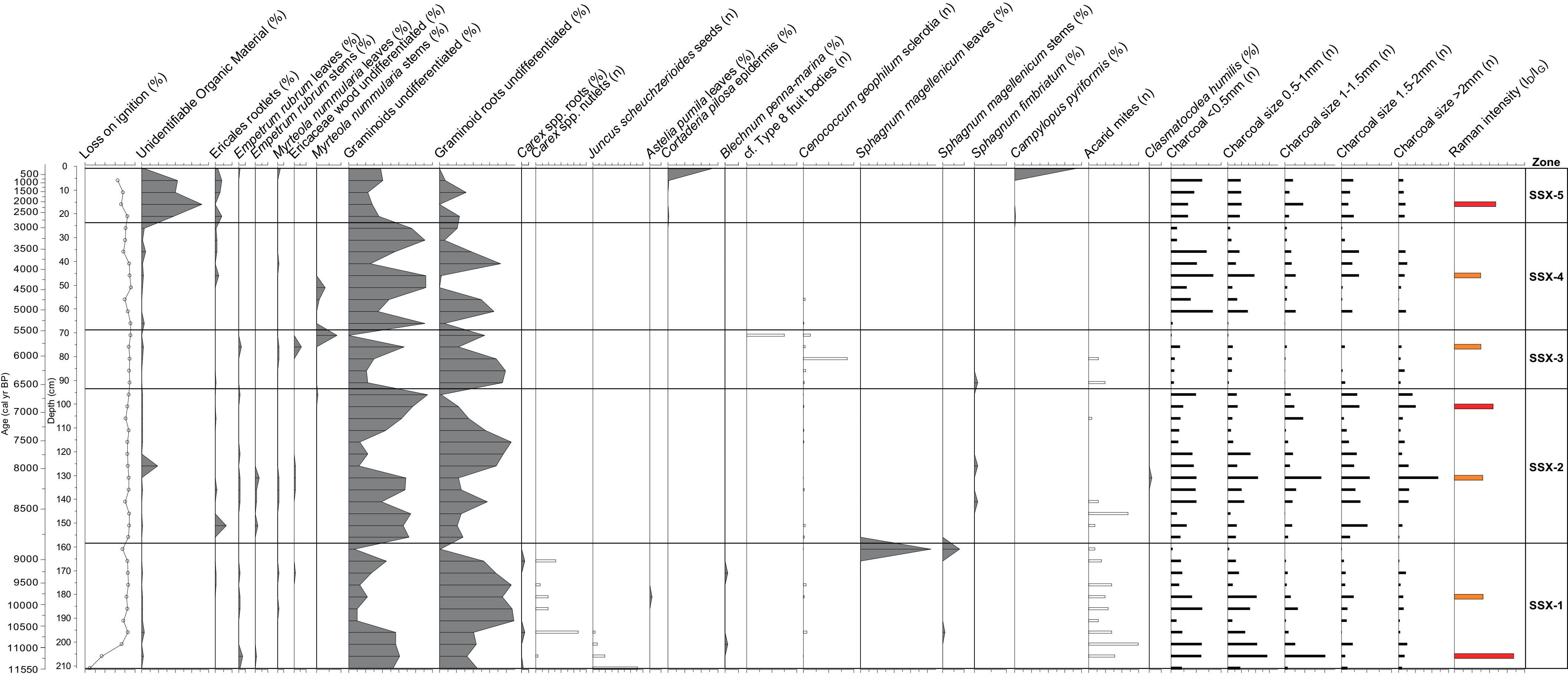

Loss on ignition (%)
Unidentifiable Organic Material (%)
Ericales rootlets (%)
Empetrum rubrum leaves (%)
Empetrum rubrum stems (%)
Myrteola nummularia leaves (%)
Ericaceae wood undifferentiated (%)
Myrteola nummularia stems (%)
Graminoids undifferentiated (%)
Graminoid roots undifferentiated (%)
Carex spp. roots (%)
Carex spp. nutlets (n)
Juncus scheuchzerioides seeds (n)
Astelia pumila leaves (%)
Cortaderia pilosa epidermis (%)
Blechnum penna-marina (%)
cf. Type 8 fruit bodies (n)
Cenococcum geophilum sclerotia (n)
Sphagnum magellenicum leaves (%)
Sphagnum magellenicum stems (%)
Sphagnum fimbriatum (%)
Campylopus pyriformis (%)
Acarid mites (n)
Clasmatocolea humilis (%)
Charcoal <0.5mm (n)
Charcoal size 0.5-1mm (n)
Charcoal size 1-1.5mm (n)
Charcoal size 1.5-2mm (n)
Charcoal size >2mm (n)
Raman intensity (I_D/I_G)
Zone
SSX-5
SSX-4
SSX-3
SSX-2
SSX-1
Age (cal yr BP)
500
1000
1500
2000
2500
3000
3500
4000
4500
5000
5500
6000
6500
7000
7500
8000
8500
9000
9500
10000
10500
11000
11550
Depth (cm)
0
10
20
30
40
50
60
70
80
90
100
110
120
130
140
150
160
170
180
190
200
210
60 80
0 20 40 60 80
0 20
0 5
0 10
0 5
0 10
0 20
0 20 40 60 80
0 20 40 60 80
0 5
0 10 20
0 10 20
0 5
0 20 40 60
0 5
0 2000
0 100
0 20 40 60 80
0 10
0 10
0 20 40 60 80
0 5 10 15
0 5
0 500
0 100 300
0 100 200
0 50
0 50 100
0 0.2 0.4 0.6 0.8

Figure 4

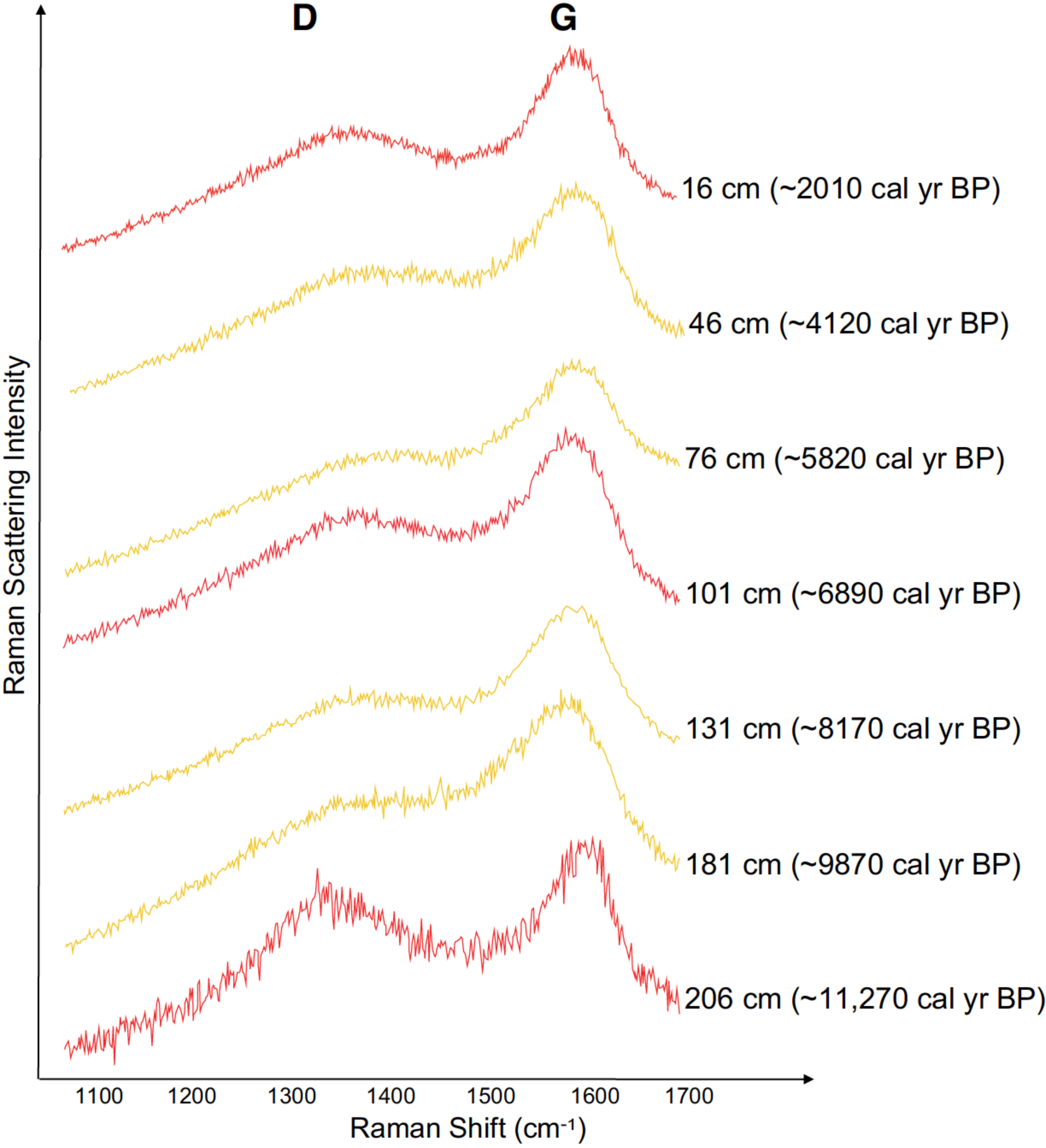
D
G
16 cm (~2010 cal yr BP)
46 cm (~4120 cal yr BP)
76 cm (~5820 cal yr BP)
101 cm (~6890 cal yr BP)
131 cm (~8170 cal yr BP)
181 cm (~9870 cal yr BP)
206 cm (~11,270 cal yr BP)
Raman Scattering Intensity
1100
1200
1300
1400
1500
1600
1700
Raman Shift (cm-1)

Figure 5

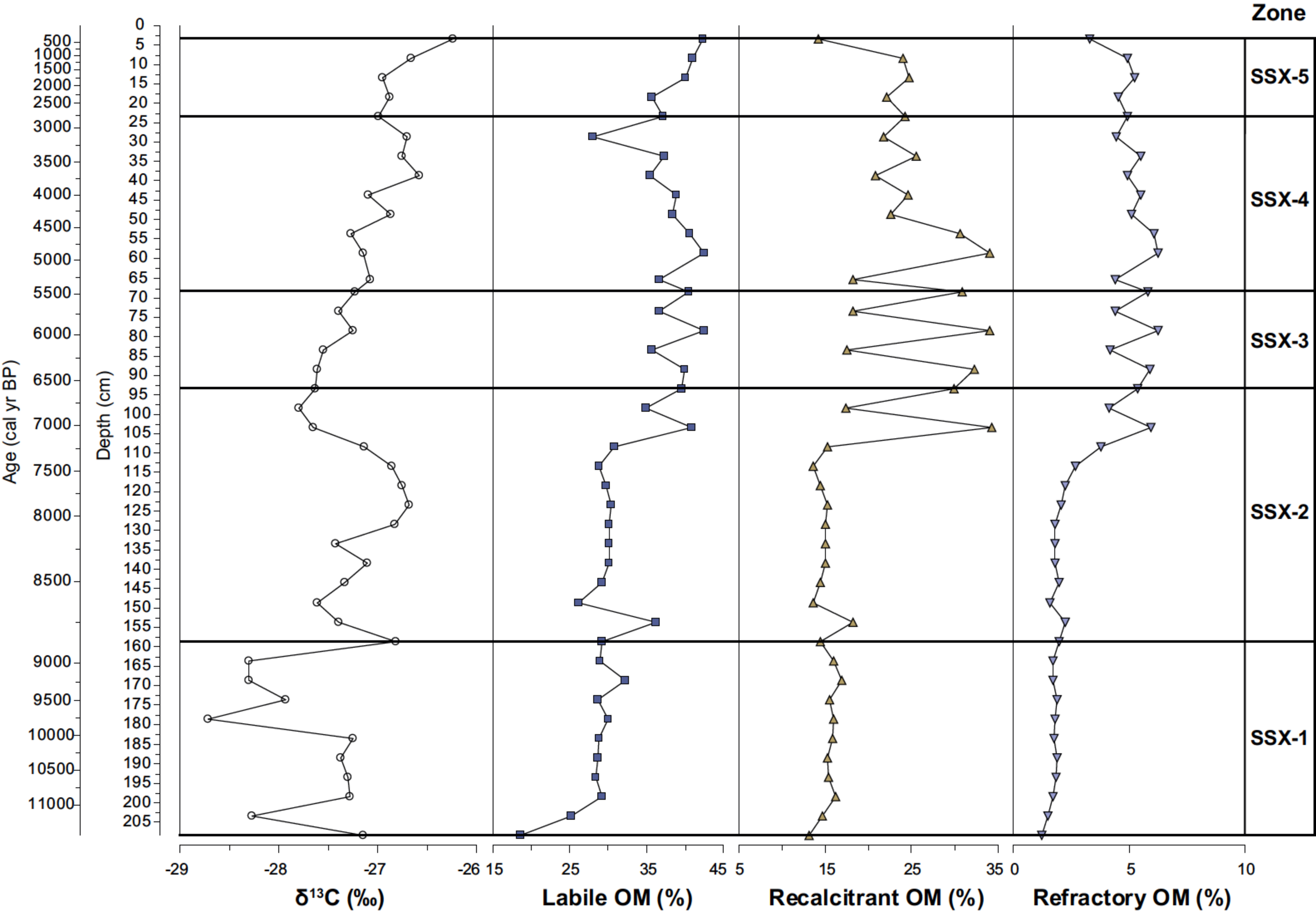
Zone
SSX-5
SSX-4
SSX-3
SSX-2
SSX-1
Age (cal yr BP)
500
1000
1500
2000
2500
3000
3500
4000
4500
5000
5500
6000
6500
7000
7500
8000
8500
9000
9500
10000
10500
11000
Depth (cm)
0
5
10
15
20
25
30
35
40
45
50
55
60
65
70
75
80
85
90
95
100
105
110
115
120
125
130
135
140
145
150
155
160
165
170
175
180
185
190
195
200
205
-29
-28
-27
-26
δ13C (‰)
15
25
35
45
Labile OM (%)
5
15
25
35
Recalcitrant OM (%)
0
5
10
Refractory OM (%)